Boosting subdominant neutralizing antibody responses with a computationally designed epitope-focused immunogen

Authors:

Sesterhenn F[1,2], Galloux M[3], Vollers SS[1], Csepregi L[4], Yang C[1,2], Descamps D[3], Bonet J[1,2], Friedensohn S[4], Gainza P[1,2], Corthésy P[1], Chen M[5], Rosset S[1], Rameix-Welti MA[6,7], Eléouët JF[3], Reddy ST[4], Graham BS[5], Riffault S[3] & Correia BE[1,2,*].

Affiliations:

[1] Institute of Bioengineering, École Polytechnique Fédérale de Lausanne, Lausanne CH-1015, Switzerland.
[2] Swiss Institute of Bioinformatics (SIB), Lausanne CH-1015, Switzerland.
[3] Unité de Virologie et Immunologie Moléculaires (UR892), INRA, Université Paris-Saclay, 78352, Jouy-en-Josas, France.
[4] Department of Biosystems Science and Engineering, ETH Zurich, Basel, Switzerland.
[5] Viral Pathogenesis Laboratory, Vaccine Research Center, National Institute of Allergy and Infectious Diseases, National Institutes of Health, Bethesda, MD, United States.
[6] UMR1173, INSERM, Université de Versailles St. Quentin, 78180 Montigny le Bretonneux, France.
[7] AP-HP, Laboratoire de Microbiologie, Hôpital Ambroise Paré, 92104, Boulogne-Billancourt, France.
[*] Corresponding author: bruno.correia@epfl.ch

Abstract

Throughout the last decades, vaccination has been key to prevent and eradicate infectious diseases. However, many pathogens (e.g. Respiratory Syncytial Virus (RSV), Influenza, Dengue and others) have resisted vaccine development efforts, largely due to the failure to induce potent antibody responses targeting conserved epitopes. Deep profiling of human B-cells often reveals potent neutralizing antibodies that emerge from natural infection, but these specificities are generally subdominant (i.e., are present in low titers). A major challenge for next-generation vaccines is to overcome established immunodominance hierarchies and focus antibody responses on crucial neutralization epitopes. Here, we show that a computationally designed epitope-focused immunogen presenting a single RSV site targeted by Palivizumab elicits superior site II epitope-specific responses compared to the RSV prefusion protein. In addition, the epitope-focused immunogen efficiently boosts antibodies targeting the Palivizumab epitope, resulting in enhanced neutralization. Overall, we show that epitope-focused immunogens can boost subdominant neutralizing antibody responses *in vivo* and reshape established antibody hierarchies.

Introduction

The development of vaccines has proven to be one of the most successful medical interventions to reduce the burden of infectious diseases (*1*), and their correlate of protection is the induction of neutralizing antibodies (nAbs) that block infection (*2*).

In recent years, advances in high-throughput B-cell technologies have revealed a plethora of potent nAbs for different pathogens which have resisted the traditional means of vaccine development for several decades, including HIV-1 (*3*), Influenza (*4*), Respiratory Syncytial Virus (RSV) (*5, 6*), Zika (*7, 8*), Dengue (*9*) and others (*10-12*). A major target of these nAb responses is the pathogens fusion protein, which drives the viral and host cell membrane fusion while undergoing a conformational rearrangement from a prefusion to a postfusion state (*13*) . Many of these nAbs have been structurally characterized in complex with their target, unveiling the atomic details of neutralization epitopes (*7, 14, 15*). Together, these studies have provided comprehensive antigenic maps of the viral fusion proteins which delineate epitopes susceptible to antibody-mediated neutralization and provide a roadmap for rational and structure-based vaccine design approaches.

The conceptual framework to leverage neutralizing antibody-defined epitopes for vaccine development is commonly referred to as reverse vaccinology (*16, 17*). Although reverse vaccinology-inspired approaches have yielded a number of exciting advances in the last decade, the design of immunogens that elicit such focused antibody responses remains challenging. Successful examples of structure-based immunogen design approaches include conformational stabilization of RSVF in its prefusion state, which induces superior serum neutralization titers when compared to immunization with F in the postfusion conformation (*18*). In the case of Influenza, several epitopes targeted by broadly neutralizing antibodies (bnAbs) were identified within the hemagglutinin (HA) stem domain, and an HA stem-only immunogen elicited a broader neutralizing antibody response than full-length HA (*19, 20*). Commonly, these approaches have aimed to focus antibody responses on specific conformations or subdomains of viral proteins. In a more aggressive approach, Correia et al. (*21*) computationally designed a synthetic immunogen presenting the RSV antigenic site II (Figure 1a), and provided a proof-of-principle for the induction of RSV neutralizing activity mediated by a single epitope in non-human primates.

RSV, among other pathogens, strikingly illustrates the major need to be able to elicit epitope-focused antibody responses. While the reasons for the failure of 1960's formalin-inactivated RSV vaccine are not fully clear, several reports have suggested that the induction of antibodies targeting non-neutralizing and structurally altered neutralization epitopes may have played a role in the disease enhancement observed upon later infection (*22-24*). Despite more than 50 years of intensive research, a licensed vaccine has remained elusive, and RSV-induced severe lower respiratory tract infections continue to cause more than three million hospitalizations annually (*25*). Thus far, the only prophylactic therapy for individuals at high risk for severe RSV disease is passive immunization with Synagis®, a monoclonal antibody targeting antigenic site II of RSVF (*25*).

The absence of a potent and long-lasting immune response upon natural infection is a major challenge associated with RSV, Influenza virus and other pathogens. While single exposure to pathogens like Poliovirus confers life-long immunity, RSV, Influenza and other pathogens have developed mechanisms to subvert the development of a durable and potent neutralizing antibody response, thereby allowing such pathogens to infect humans repeatedly throughout their lives (*26*). One of the major factors hindering the induction of long-lasting protection after the first infection is related to the antibody specificities induced. Upon exposure to the pathogen, the human antibody responses predominantly target non-neutralizing or strain-specific antigenic sites, whereas potent bnAbs are subdominant (*27*). This phenomenon is generally referred to as B-cell immunodominance, which describes the unbalanced immunogenicity of certain antigenic sites within an antigen, favoring strain-specific, variable, non-neutralizing epitopes to the detriment of conserved, neutralization-sensitive epitopes (*28*). The factors that determine the antigenicity of specific epitopes remain unclear, making the categorization of immunodominant and subdominant epitopes an empirical classification based on serological analysis. Importantly, the presence of high levels of antibodies directed against immunodominant epitopes can sterically mask surrounding subdominant epitopes that may be targeted by bnAbs, preventing the immune system from mounting productive antibody responses against subdominant epitopes, and potentially limiting vaccination efficacy (*27-30*).

107 The immunodominance hierarchy is established within the germinal center, where B-
108 cells undergo a binding affinity-based competition for available antigen and
109 subsequently initiate a clonal expansion stage, ultimately becoming long-lived plasma
110 cells or memory B-cells (*31*). Controlling this competition and driving antibody
111 responses towards the increased recognition of subdominant, neutralizing epitopes is
112 of primary importance to enable development of novel vaccines to fight pathogens
113 which have resisted traditional strategies. One of the few strategies to guide antibody
114 maturation was tested in the HIV field and is referred to as germline targeting, which
115 relies upon the activation and expansion of rare but specific B-cell lineages in naïve
116 individuals (*32, 33*). In contrast, under conditions of pre-existing immunity acquired
117 during natural infection or previous vaccination, the challenge is to manipulate already
118 established B-cell immunodominance hierarchies and reshape serum antibody
119 responses towards desired specificities. In an indirect approach towards increasing
120 subdominant B-cell populations, Silva et al. (*34*) have shown that the targeted
121 suppression of immunodominant clones during an active germinal center reaction can
122 allow subdominant B-cell populations to overtake the germinal center response. Other
123 approaches have used heterologous prime-boost immunization regimens with either
124 alternative viral strains or rationally modified versions of the priming immunogen (*35-*
125 *38*) in order to steer antibody responses towards more conserved domains. However,
126 leveraging structural information of defined neutralization epitopes to guide bulk
127 antibody responses towards specific, well-characterized single epitopes remains an
128 unmet challenge.
129
130 Here, we investigate whether, under conditions of pre-existing immunity, a
131 computationally designed immunogen presenting a single epitope is able to reshape
132 serum antibody responses towards increased recognition of a specific neutralizing
133 epitope. For these studies, we used an optimized formulation and resurfaced version
134 of the previously designed RSV site II epitope-scaffold targeted by the monoclonal
135 antibody Palivizumab (*21*), the only FDA-approved prophylactic measure against RSV
136 infection.
137
138 We show that an optimized, multivalent presentation of an RSV antigenic site II
139 scaffold elicits superior levels of epitope-specific antibodies compared to prefusion
140 RSVF in naïve mice, indicating that the immunodominance of a particular epitope can

be altered through its presentation in a distinct molecular context. We further used the site II scaffold as a boosting immunogen in animals primed with prefusion RSVF, mimicking a scenario of pre-existing immunity against RSVF. Whereas homologous boosting immunizations with prefusion RSVF failed to increase site II-specific antibodies, we found that heterologous boosts with an epitope scaffold nanoparticle enhanced serum responses towards this *bona fide* vaccine target, and that the boosted antibodies neutralized RSV *in vitro*. For the first time, we provide compelling evidence that synthetic immunogens comprising a single epitope can efficiently enhance subdominant neutralizing antibody responses *in vivo* and redirect specificities in bulk antibody responses. Such a strategy may present an important alternative for pathogens where future vaccines are required to reshape pre-existing immunity and elicit finely tuned antibody specificities.

153 **Results**

154

155 Design of an RSV-based nanoparticle displaying a site II epitope-focused immunogen

156 In a previous study, a computationally-designed, RSV site II epitope-scaffold
157 nanoparticle was shown to elicit serum neutralization activity in non-human primates
158 (NHPs) (*21*). Despite the fact that very potent monoclonal antibodies were isolated
159 from the immunized NHPs, the neutralization potency at serum level was modest,
160 indicating low titers of the potent antibodies. Therefore, our first aim was to take the
161 best previously tested immunogen (FFL_001) and further optimize the immunogen
162 delivery and immunization conditions to maximize the induction of site II-specific
163 antibodies. A comparative study of four different adjuvants revealed that Alhydrogel®,
164 an adjuvant approved for human use, yielded highest overall immunogenicity and
165 elicited antibodies cross-reactive with prefusion RSVF in four out of five mice
166 (Supplementary Fig. 1).

167

168 Next, we sought to develop an improved, easily produced nanoparticle to multimerize
169 the epitope-scaffold for efficient B-cell receptor crosslinking. Previously, Correia et al.
170 (*21*) employed a chemical conjugation strategy of FFL_001 to a Hepatitis-B core
171 antigen based nanoparticle, which resulted in a difficult construct with a laborious
172 purification process. Recently, several studies have reported the use of RSV
173 nucleoprotein (RSVN) as a nanoparticle platform for immunogen presentation (*39, 40*).
174 When expressed in *E. coli*, RSVN forms nanorings, 17 nm in diameter, containing 10
175 or 11 RSVN protomers (*41*). We reasoned that RSVN would be an ideal particle
176 platform to multimerize an RSV epitope scaffold, as RSVN contains strong, RSV-
177 directed T-cell epitopes (*40*). However, our initial attempts to genetically fuse FFL_001
178 to RSVN yielded poorly soluble proteins that rapidly aggregated after purification. We
179 therefore employed structure-based protein resurfacing (*42*), attempting to improve
180 the solubility of this site II epitope-scaffold when arrayed in high density on RSVN. To
181 guide our resurfacing design process, we leveraged information from a sequence
182 homolog of the ribosomal recycling factor (PDB: 1ISE), the structural template
183 originally used to design FFL_001. Based on a sequence alignment of the mouse
184 homolog (NCBI reference: NP_080698.1) and FFL_001, we exchanged the FFL_001
185 amino acids for the mouse sequence homolog and used Rosetta Fixed Backbone
186 Design (*43*) to ensure that the mutations were not energetically unfavorable, resulting

187 in 38 amino acid substitutions (34.2% overall). We named this variant FFLM, whose
188 expression yields in *E. coli* showed a five-fold increase when compared to FFL_001,
189 and it was confirmed to be monomeric in solution (Supplementary Fig. 2).
190
191 To confirm that the resurfacing did not alter the epitope integrity, we measured the
192 binding affinities of FFLM to Motavizumab, a high-affinity variant of Palivizumab (*44*),
193 and to a panel of human site II nAbs previously isolated (*5*) using surface plasmon
194 resonance (SPR). All antibodies bound with high affinity to FFLM, indicating broad
195 reactivity of this immunogen with a diverse panel of human nAbs (Figure 1b).
196 Interestingly, the tested nAbs showed approximately one order of magnitude higher
197 affinity to the epitope-scaffold as compared to prefusion RSVF, suggesting that the
198 epitope is properly presented and likely further stabilized in a relevant conformation.
199
200 Importantly, the FFLM-RSVN fusion protein expressed with high yields in *E. coli* (>10
201 mg/liter), forming a nanoring particle, dubbed NRM, that was monodisperse in solution
202 with a diameter of approximately 21 nm (Figure 1c). Although we cannot fully
203 rationalize the factors that contributed to the solubility improvement upon
204 multimerization, our strategy to transplant surface residues from a sequence homolog
205 to synthetic proteins may prove useful to enhance the solubility of other
206 computationally designed proteins.
207

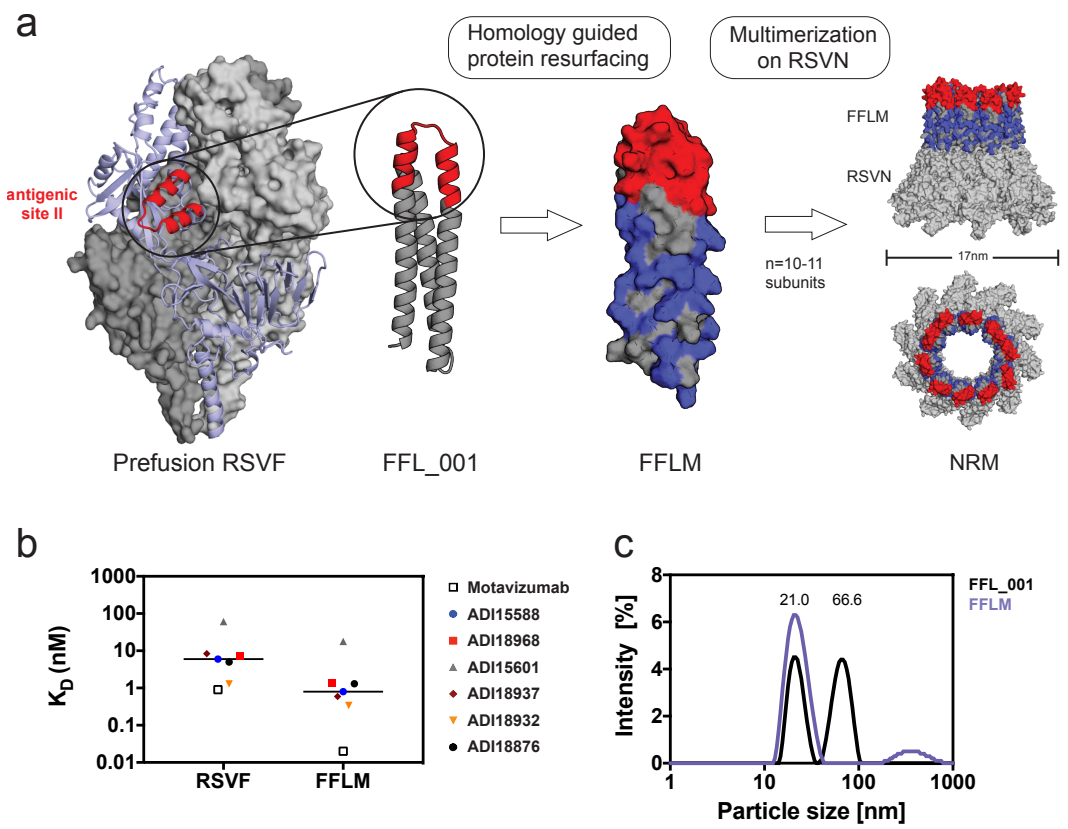

Figure 1:

Design of an RSV-based nanoparticle displaying a site II epitope-focused immunogen. a) Structural model of the prefusion RSVF trimer (PDBID: 4JHW), with two subunits shown as a grey surface and one subunit shown as light blue cartoon representation with the epitope targeted by Palivizumab (antigenic site II) highlighted in red. FFL_001 was previously designed to present the site II epitope in a computationally designed scaffold. FFLM was designed by evolution-guided resurfacing, where changes in amino acid identity are highlighted in blue. FFLM was genetically fused to the N-terminus of the RSV nucleoprotein (RSVN), resulting in a high-density array of the epitope scaffold, as shown by the structural model (based on PDBID: 2WJ8). **b)** Binding affinities of site II-specific human nAbs measured by SPR. K_Ds were measured with RSVF/FFLM immobilized as ligand and antibody fabs as analyte. nM = nanomolar. **c)** Dynamic light scattering (DLS) profiles for FFL_001 and FFLM fused to RSVN. The FFL_001-RSVN fusion protein formed higher-order oligomers in solution (66.6 nm of median diameter), whereas the resurfaced FFLM-

225 RSVN fusion protein (NRM) was monodisperse with a median diameter of 21 nm. nm
226 = nanometer.
227
228 NRM enhances the induction of site II-specific antibodies
229 We next tested the immunogenicity of the site II scaffold nanoring and its ability to elicit
230 site II-specific antibodies. Three groups of ten mice were subjected to three
231 immunizations with 10 μg of NRM, monomeric FFLM and prefusion RSVF (*45*), which
232 is currently the leading immunogen for an RSV vaccine (Figure 2a). Based on the
233 results of our adjuvant screen (Supplementary Fig. 1), all the immunogens were
234 formulated in Alhydrogel, an adjuvant approved for human use. As compared to FFLM,
235 NRM showed a higher overall immunogenicity (directed both against RSVN and
236 FFLM) (Figure 2b).
237
238 A key aspect of epitope-focused vaccines is to understand how much of the antibody
239 response targets the viral epitope presented to the immune system. Therefore, we
240 sought to measure the site II-specific antibody titers elicited by NRM and FFLM and
241 compare these epitope-specific antibody responses to those elicited by prefusion
242 RSVF. Using an SPR competition assay to measure site II-specific antibodies in sera
243 (described in methods), we observed that NRM elicited site II-specific antibody
244 responses superior to those elicited by RSVF (Figure 2c). This was surprising, given
245 that the ratio of site II epitope surface area to overall immunogen surface is similar in
246 both NRM and RSVF (Supplementary Fig. 2). To confirm this finding through a direct
247 binding assay rather than a competitive format, we measured the binding levels of
248 sera to the site II epitope in a peptide ELISA, where the site II peptide was immobilized
249 on streptavidin-coated wells. Consistent with the previous experiment, we found that
250 NRM elicited two orders of magnitude higher site II-specific responses than RSVF
251 (Figure 2d). Together, these data validated NRM as our lead immunogen to induce
252 high levels of site II-specific antibodies in mice.
253

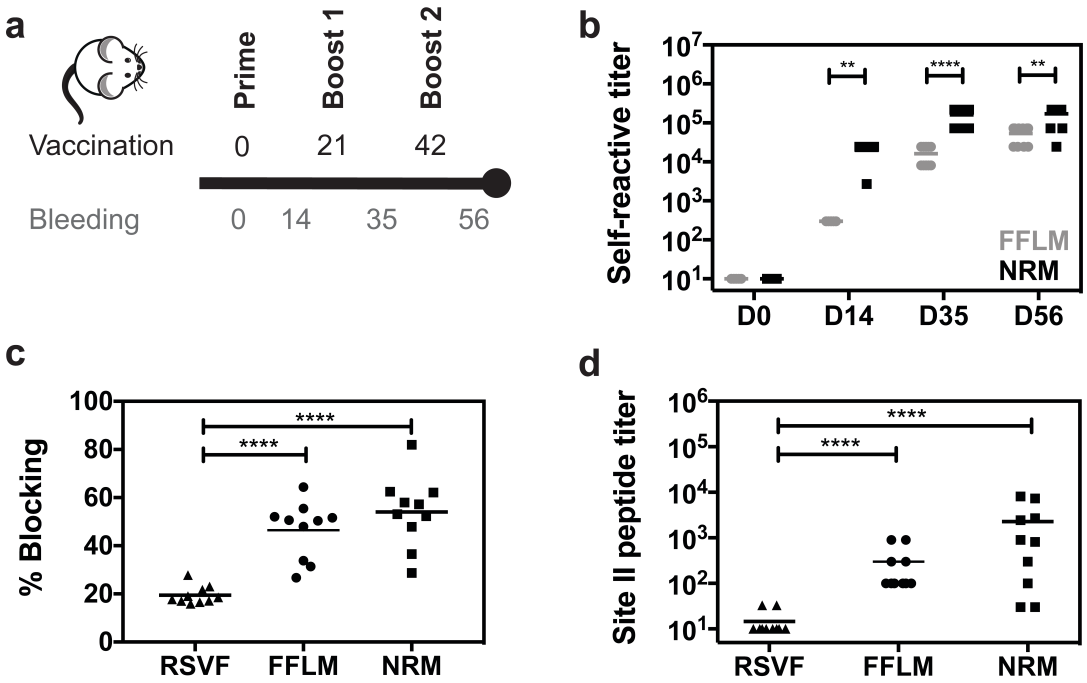

Figure 2:
Immunogenicity and quantification of site II-specific antibody responses. a) Immunization scheme. Balb/c mice were immunized three times on days 0, 21 and 42, and blood was drawn 14 days after each vaccination. **b)** Serum antibody titers elicited by FFLM and NRM at different timepoints measured by ELISA against the respective immunogen. NRM shows significantly increased immunogenicity at day 14, 35 and 56 relative to FFLM. **c)** SPR competition assay with Motavizumab. Day 56 sera of mice immunized with RSVF, FFLM or NRM was diluted 1:100 and SPR response units (RU) were measured on sensor chip surfaces containing the respective immunogen. Motavizumab binding sites were then blocked by saturating amounts of Motavizumab, and the residual serum response was measured to calculate the serum fraction competed by Motavizumab binding. Mice immunized with FFLM or NRM show significantly higher levels of serum antibodies that are competed by Motavizumab binding. **d)** Site II-specific serum titers at day 56 from mice immunized with RSVF, FFLM and NRM, measured by ELISA against site II peptide. Three immunizations with prefusion RSVF elicited low levels of site II-specific antibodies, whereas FFLM and NRM vaccinations yielded significantly higher peptide-specific serum titers. Data shown are derived from at least two independent experiments, each sample assayed

273 in duplicate. Statistical comparisons were calculated using two-tailed Mann-Whitney
274 U tests. ** indicates $p < 0.01$, *** indicates $p < 0.0001$, **** $p < 0.0001$

275 NRM induces low levels of RSVF cross-reactive antibodies with low neutralization
276 potency
277 Given the substantial site II-specific serum titers elicited by NRM in mice, we
278 investigated whether these antibodies cross-reacted with prefusion RSVF and were
279 sufficient to neutralize RSV *in vitro*.
280
281 Following three immunizations with NRM, all the mice (n=10) developed detectable
282 serum cross-reactivity with prefusion RSVF (mean serum titer = 980) (Figure 3a).
283 Unsurprisingly, the overall quantity of prefusion RSVF cross-reactive antibodies
284 elicited by immunization with an immunogen presenting a single epitope is more than
285 two orders of magnitude lower than those of mice immunized with prefusion RSVF,
286 which comprises at least six antigenic sites (*5*). Similarly, a B-cell ELISpot revealed
287 that NRM-immunized mice presented prefusion RSVF-reactive antibody secreting
288 cells, but their frequency was approximately one order of magnitude lower than upon
289 immunization with prefusion RSVF (Figure 3c).
290
291 The major determinant for antibody specificity is attributed to the heavy chain CDR3
292 region (HCDR3) (*46*). While for certain classes of nAbs, the antibody lineages and
293 their sequence features are well-defined (e.g. HIV neutralizing VRC01 class
294 antibodies (*47*), or RSV neutralizing MPE8-like antibodies (*48*)), antibodies targeting
295 RSV antigenic site II seem to be derived from diverse precursors and do not show
296 HCDR3 sequence convergence in humans (*5*). While we did not expect to find
297 dominant lineages or HCDR3 sequence patterns in mice, we used next-generation
298 antibody repertoire sequencing (*49*) to ask whether NRM could elicit antibodies with
299 similar sequence signatures to those elicited by prefusion RSVF. Indeed, we found
300 300 clonotypes, defined as antibodies derived from the same VH gene with the same
301 HCDR3 length and 80% sequence similarity, that overlapped between NRM and the
302 prefusion RSVF immunized cohort, suggesting that at the molecular level, relevant
303 antibody lineages can be activated with the NRM immunogen (Supplementary Figure
304 3). Notably, nine out of the 20 most expanded clonotypes in the NRM cohort were also
305 present in mice immunized with prefusion RSVF, albeit not as expanded (Figure 3b).
306 This finding might reflect the enrichment of site II specific antibodies in the NRM cohort
307 (Figure 2d).
308

309 We further investigated whether these low levels of prefusion RSVF-binding
310 antibodies were sufficient to neutralize RSV *in vitro*. While three immunizations with
311 prefusion RSVF elicited potent RSV-neutralizing serum titers (mean IC_{50}= 10,827), for
312 NRM we only detected low levels of RSV-neutralizing serum activity in three out of ten
313 mice (Figure 3d). This result is consistent with Correia *et al*. (*21*), who observed no
314 serum neutralization in mice, but succeeded in inducing nAbs in NHPs with prior RSV
315 seronegativity.
316
317 Altogether, we concluded that despite NRM's superior potential to induce high levels
318 of site II-specific antibodies, the majority of antibodies activated from the naïve
319 repertoire is unable to potently neutralize RSV *in vitro*. A potential explanation,
320 stemming from structural comparison between the epitope-focused immunogen
321 (FFLM) and RSVF, is that although epitope-specific antibodies are abundantly elicited
322 by NRM, these antibodies do not recognize the site II epitope in its native RSVF
323 quaternary environment in the prefusion conformation, or on virions in sufficient
324 amounts and with high enough affinity to potently neutralize RSV.
325

Fig. 3

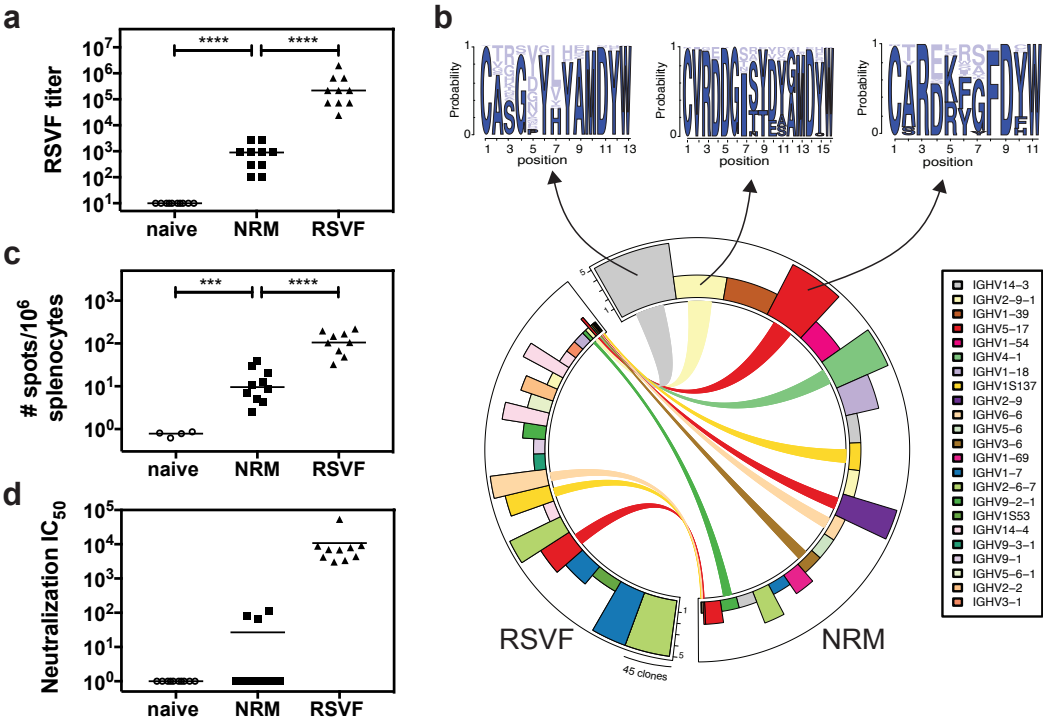

Figure 3:

RSVF cross-reactivity and serum neutralization. **a)** NRM elicits prefusion RSVF cross-reactive antibodies, which are two orders of magnitude lower compared to prefusion RSVF immunization. Mice immunized only with adjuvant (naïve) do not show RSVF cross-reactivity. **b)** Next-generation sequencing of antibody repertoire. Antibody variable heavy chains of mice immunized with RSVF or NRM (5 mice per cohort) were sequenced and grouped into clonotypes. Circos plot showing the 20 most expanded clonotypes from both cohorts, with identical clonotypes connected. Height of bars indicates number of mice that showed the respective clonotype, width represents the clonal expansion within a clonotype (i.e. the number of clones grouped into the respective clonotype). Three clonotypes that occurred both in the RSVF and the NRM cohort, but were expanded within the NRM cohort were analyzed for their HCDR3 sequence profile, as shown by sequence logo plots (top). Dark blue color represents amino acid identities that occurred in RSVF cohort, light blue color represents amino acids uniquely found following NRM immunization. The frequency of each amino acid in the NRM cohort is indicated by the size of the letter. **c)** B-cell ELISpot of mouse splenocytes to quantify prefusion RSVF-specific antibody secreting cells (ASC).

Number of ASCs per 10^6 splenocytes that secrete prefusion RSVF-specific antibodies following three immunizations with adjuvant only (naïve), NRM or prefusion RSVF **d)** RSV neutralizing activity of mouse sera from day 56 shown as neutralization IC_{50}. Three out of ten mice immunized with NRM showed detectable RSV neutralizing activity, whereas all mice immunized with prefusion RSVF neutralized RSV (mean IC_{50} = 10,827). Data shown are from one out of two independent experiments. Statistical comparisons were calculated using two-tailed Mann-Whitney U tests. *** indicates $p < 0.001$, **** indicates $p < 0.0001$.

355 NRM boosts site II-specific antibodies under conditions of pre-existing immunity
356 While RSV vaccination studies in naïve animal models are an important first step to
357 validate novel immunogens, two important human target populations for RSV
358 vaccination are pregnant women and the elderly. These two groups are seropositive
359 for RSVF due to life-long recurrent infections and have a basal level of RSV nAbs (*50*).
360 We hypothesized that the high affinity of the epitope scaffold towards a panel of site
361 II- specific nAbs, together with the ability to elicit high titers of site II-specific antibodies
362 *in vivo*, could make the NRM an efficient immunogen to recall RSVF primed site II-
363 specific B-cells, thereby achieving an enhanced and focused neutralization response.
364
365 Our initial homologous prime-boost immunization studies with prefusion RSVF
366 showed that site II-specific responses were subdominant (Figure 2c and 2d). Given
367 that subdominance is a common immunological phenotype for many of the
368 neutralization epitopes that are relevant for vaccine development (*51*), we sought to
369 test if NRM could boost subdominant site II-specific antibody lineages that should
370 ultimately be functional and recognize the epitope in the tertiary environment of
371 prefusion RSVF. To test this hypothesis, we designed a mouse immunization
372 experiment with three cohorts, as outlined in Figure 4a. Following a priming
373 immunization with RSVF, cohort (1) was boosted with adjuvant only ("prime only"),
374 cohort (2) received two boosting immunizations with prefusion RSVF ("homologous
375 boost"), and cohort (3) received two boosts with NRM ("heterologous boost").
376
377 A comparison between prefusion RSVF immunized groups prime only and
378 homologous boost revealed that the two additional boosting immunizations with RSVF
379 only slightly increased overall titers of prefusion RSVF-specific antibodies ($p = 0.02$,
380 Mann-Whitney), indicating that a single immunization with adjuvanted RSVF is
381 sufficient to induce close to maximal serum titers against RSVF (Figure 4b). Following
382 the heterologous boost with NRM, overall RSVF specific antibody titers remained
383 statistically comparable to the prime only group ($p = 0.22$, Mann-Whitney).
384
385 Next, we quantified the site II-specific endpoint serum titers in a peptide ELISA format
386 (Figure 4c). Interestingly, the homologous boost with prefusion RSVF failed to
387 increase site II-specific antibody levels, reducing the responses directed to site II to
388 the lower limit of detection by ELISA. This result is yet another example of the

underlying complexity inherent to the fine specificity of antibody responses elicited by immunogens and how important specificities can be dampened throughout the development of an antibody response. In contrast to the homologous boost, the heterologous boost with NRM significantly increased site II peptide-specific serum titers ($p < 0.0001$, Mann-Whitney).

In order to understand whether this increase relied at least partially on an actual recall of antibodies primed by RSVF, or rather on an independent antibody response irrelevant for RSVF binding and RSV neutralization, we dissected the epitope specificity within the RSVF-specific serum response. In an SPR competition assay, a significantly higher fraction ($p = 0.02$, Mann-Whitney) of prefusion RSVF-reactive antibodies were competed by Motavizumab in mouse sera primed with prefusion RSVF and boosted with NRM (mean % competition = 37.5 ± 14.5%), as compared to mice immunized once or three times with prefusion RSVF (21.5% ± 12.1% or 19.5% ± 3.7%, respectively) (Figure 4d). Similarly, a competition ELISA revealed that a significantly larger fraction of overall RSVF reactivity was attributed to site II-specific antibodies upon heterologous boost, as compared to both control groups (36.1% ± 2.5% versus 22.6% ± 9.1% or 14.4% ±5.9%, respectively, $p = 0.002$ and $p < 0.0001$, Mann-Whitney). In contrast, site II-specific antibodies were significantly higher in mice that received only one as opposed to three RSVF immunizations, indicating that RSVF boosting immunizations depleted site II-specific antibody titers ($p = 0.03$, Mann-Whitney) (Figure 4e).

Together, we have shown that the serum antibody specificity can be steered towards antigenic site II by boosting with NRM under conditions of pre-existing immunity, and thereby increase site II-specific antibody levels *in vivo*. This is an important and distinctive feature of NRM compared to prefusion RSVF, which was shown to decrease Palivizumab-like antibody responses under the same conditions. These results may have broad implications on strategies to control antibody fine specificities in vaccination schemes, both for RSV and other pathogens.

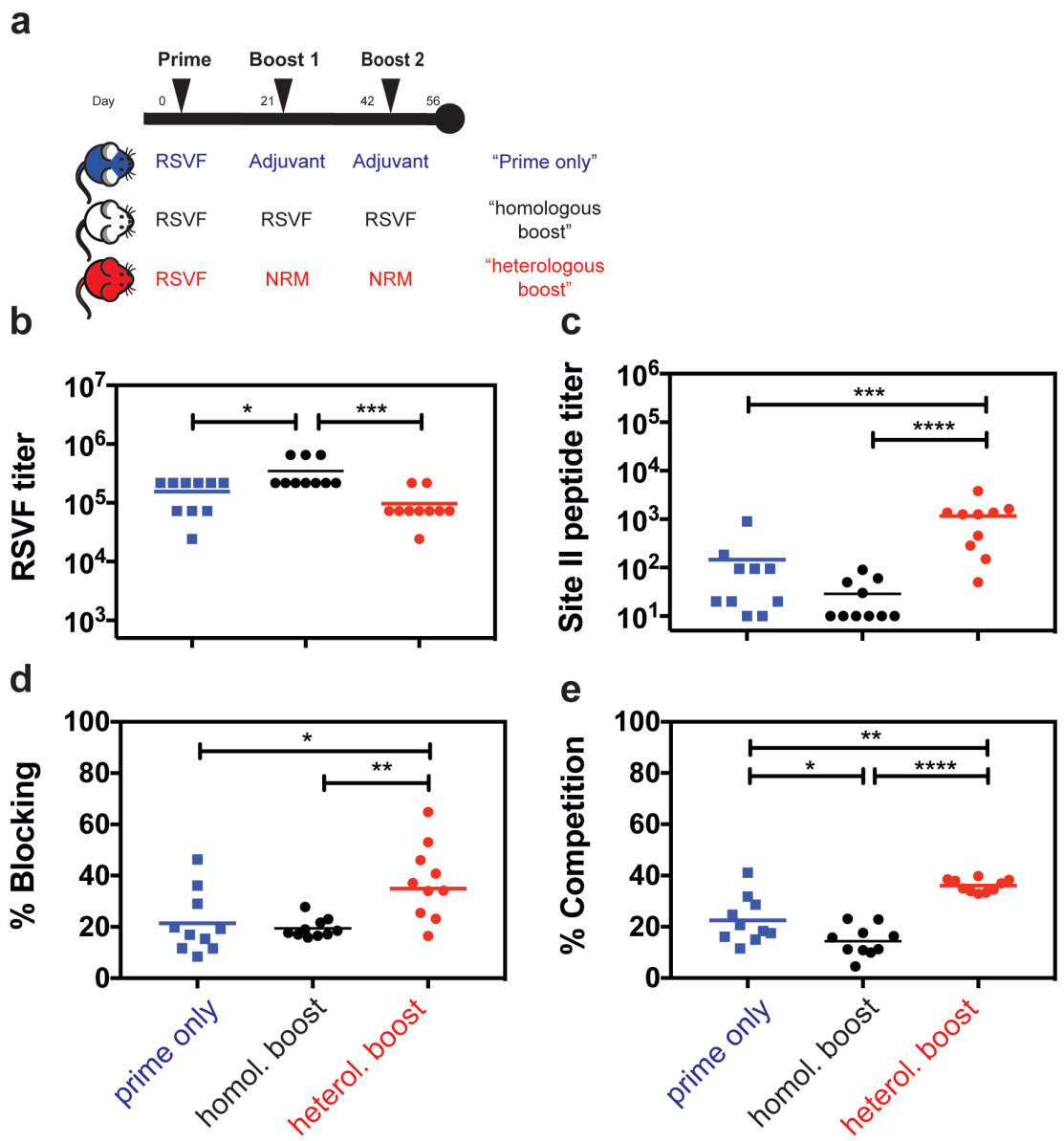

Figure 4:

Heterologous prime boost reshapes antibody responses enhancing levels of site II specific antibodies. a) Heterologous prime-boost study groups. Three mouse cohorts were immunized with either 1x RSVF ("prime only"), 3x RSVF ("homologous boost") or 1x RSVF followed by two boosts with NRM ("heterologous boost"). **b)** Antibody titers directed against prefusion RSVF. Mice receiving homologous boosting immunizations show slightly higher RSVF-specific serum titers compared to the prime only cohort, whereas heterologous boosting yielded statistically comparable titers to the prime only group. The difference between the homologous and heterologous boost cohorts was statistically significant. **c)** Site II-specific titers measured by ELISA showed that the heterologous boost significantly increases site II-specific titers

compared to both prime and homologous boost groups. Albeit not statistically significant ($p = 0.06$), mice receiving a homologous boost had lower levels of site II-specific antibodies compared to prime only group. **d)** SPR competition assay with Motavizumab on a prefusion RSVF-coated sensor chip. Sera from indicated groups were diluted 1:100 and RSVF binding responses were quantified. Site II was then blocked with Motavizumab, and the remaining serum response quantified. The heterologous boost induced a significantly higher fraction of site II-directed antibodies competed with Motavizumab for RSVF binding, as compared to both prime only and homologous boost groups). **e)** Quantification of site II-specific responses in a competition ELISA. Binding was measured against prefusion RSVF, and the Area Under the Curve (AUC) was calculated in presence of NRM competitor, normalized to the AUC in the presence of RSVN as a control competitor. Compared to the prime only group, the homologous boost resulted in significantly lower site II-specific serum titers, confirming the trend observed in c). The heterologous boost increased the fraction of site II-targeting antibodies within the pool of prefusion RSVF-specific antibodies compared to both control groups. Data presented are from at least two independent experiments, with each sample assayed in duplicates. Statistical comparisons were calculated using two-tailed Mann-Whitney U tests. * indicates $p<0.05$, ** indicates $p < 0.01$, *** indicates $p < 0.0001$, **** $p < 0.0001$.

457 Boosted antibodies neutralize RSV *in vitro*

458 The enhanced reactivity to site II observed in the heterologous prime-boost scheme
459 led us to investigate if changing the nature of the immune response had functional
460 consequences upon RSV neutralization. Overall, we observed 2.3-fold higher serum
461 neutralization titers in mice receiving a heterologous boost (mean IC_{50}=7654)
462 compared to the prime only control group (mean IC_{50}=3275) (Figure 5a). While the
463 neutralization titer difference in these two groups (prime vs. heterologous boost) did
464 not reach statistical significance, the homologous prime boost was significantly
465 improved relative to the prime only (mean IC_{50} = 10,827 vs mean IC_{50} = 3,276) and
466 interestingly, we also did not observe a statistically significance between the
467 homologous boost and the heterologous boost cohort (mean IC_{50} = 10,827 vs. mean
468 IC_{50} = 7,654).

469

470 Next, we assessed if this increase in neutralization was driven by increased levels of
471 Palivizumab-like antibodies. We observed that site II-directed antibody levels
472 correlated with overall serum neutralization titers in the heterologous prime boost
473 group (r^2=0.76, p=0.0009) (Figure 5b), whereas prime only (r^2=0.32, p=0.09) or
474 animals receiving a homologous boost showed no such correlation (r^2 = 0.18, p=0.22)
475 (Supplementary Figure 4). To characterize the neutralizing serum activity dependence
476 on antigenic site II, we pooled mouse sera within each cohort, enriched site II-specific
477 antibodies and measured neutralization (see methods). Briefly, we incubated pooled
478 sera from each group with streptavidin beads conjugated to biotin-labeled antigenic
479 site II peptide, and eluted bound antibodies. To control for the quality of the enrichment
480 protocol, we verified by ELISA that the column flow-through was depleted of site II-
481 specific antibodies (Supplementary Figure 5).

482

483 Strikingly, mice receiving a heterologous boost showed a 15-fold increase in site II-
484 mediated neutralization as compared to mice immunized once or three times with
485 prefusion RSVF (Figure 5c). We performed the same experiment for mice immunized
486 three times with NRM and did not detect any RSV neutralization in this format. This
487 observation is consistent with the very low levels of bulk sera neutralization measured
488 in this group, indicating that NRM can only boost nAbs under conditions of pre-existing
489 immunity. In summary, we conclude that the heterologous boosting scheme with a
490 single epitope immunogen enhanced subdominant neutralizing antibody responses

directed against the antigenic site presented, and effectively redirected an antibody-based immune response *in vivo*.

494

Fig. 5

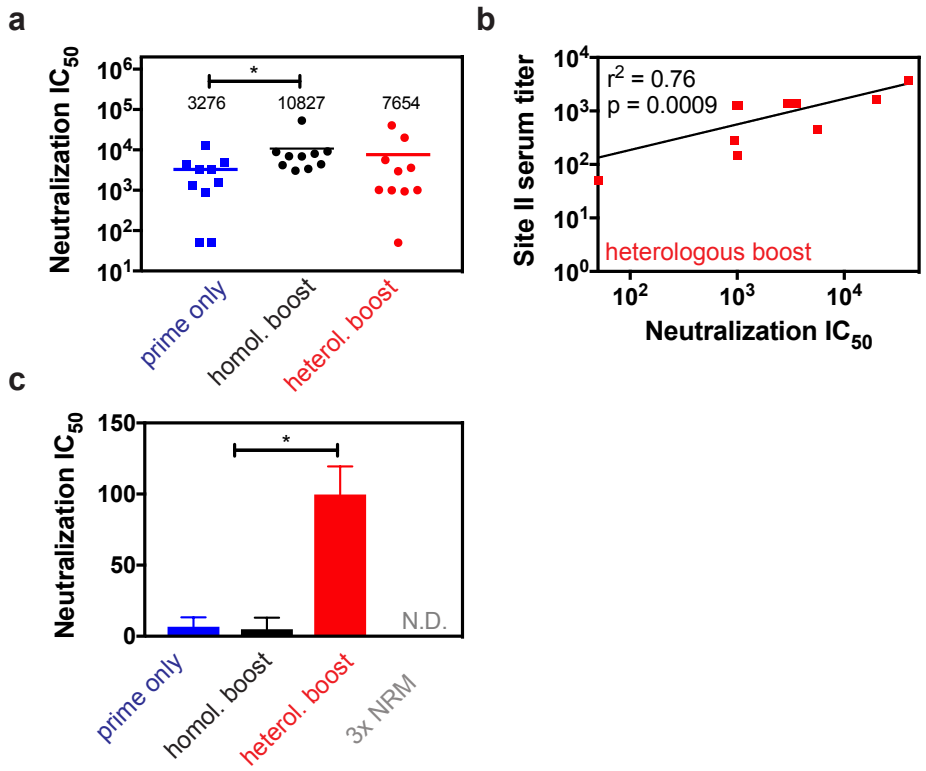

495
496 Figure 5

497 **Boosted site II-specific antibodies are functional and mediate increased**
498 **neutralization activity. a)** *In vitro* RSV neutralization IC_{50} for each group. Compared
499 to the prime only group, mice receiving a homologous boost showed increased RSV
500 neutralization titers. On average, the heterologous boost yielded a 2.3-fold increase in
501 serum neutralization titers compared to prime only, but these differences were
502 statistically not significant when compared to either group. **b)** Correlation of site II-
503 specific serum titer (measured by peptide ELISA) with RSV neutralization IC_{50} as
504 determined for each mouse within the heterologous prime boost cohort. Correlations
505 for control groups are shown in Supplementary Figure 4. Data represent the mean of
506 two independent experiments, each measured in duplicate. Pearson correlation
507 coefficient (r^2) and p-value were calculated in GraphPad Prism. **c)** Site II-specific
508 antibody fractionation revealed increased levels of nAbs. Site II-specific antibodies
509 from mouse sera were enriched in an affinity purification. Those isolated from the
510 heterologous boost group showed a 15-fold increase in RSV neutralizing activity
511 compared to both control groups. No site II-mediated neutralization was detected for
512 mice receiving three immunizations of NRM (N.D. = non-detectable). Data are

513 presented from two independent experiments, and each sample was assayed in
514 duplicate with additional controls shown in Supplementary Figure 5. Statistical
515 comparisons were calculated using two-tailed Mann-Whitney U tests. * indicates $p <$
516 0.05.

517 **Discussion**

518

519 Despite a rapid increase in our atomic-level understanding of antibody-antigen
520 interactions for various pathogens, the translation of structural information into
521 efficacious immunogens eliciting an antibody response specific to *bona fide* epitopes
522 remains a key challenge for next-generation vaccine development. In recent years,
523 numerous nAbs have been identified that target different epitopes on pre- and
524 postfusion RSVF, where prefusion-specific nAbs in particular have been proposed for
525 further clinical development and provide a plethora of valuable vaccine design targets
526 (*52*). Despite these advances, the proven clinical success of Palivizumab (*53*)
527 supports the induction of high levels of Palivizumab-like antibodies as a key route of
528 vaccine development for both naïve and RSV seropositive individuals.

529

530 Epitope scaffolds have been shown to hold great potential to elicit RSV antigenic site
531 II-specific, neutralizing antibody responses in naïve non-human primates, and an
532 elicited monoclonal antibody showed superior neutralization potency to that of
533 Palivizumab (*21*). However, a major limitation of epitope scaffolds or peptide-based
534 vaccine approaches (*54-56*) is that the quaternary environment of the epitope in its
535 viral protein is lost, and thereby the binding mode of a significant fraction of the
536 antibodies elicited is likely incompatible with the epitope in its native environment. This
537 observation is reinforced by our finding that although NRM elicited high serum levels
538 of site II-directed antibodies, only residual RSV neutralizing activity was observed,
539 which is consistent with the results of several previous studies using epitope scaffolds
540 (*56-58*). This presents a major limitation to the use of synthetic scaffolds in an epitope-
541 focused vaccine approach in naïve individuals.

542

543 However, some of the most relevant target populations for RSV vaccination (both
544 pregnant women and the elderly) have pre-existing humoral responses against RSVF,
545 including to site II (*59*). To date, boosting nAbs targeting specific epitopes under
546 conditions of pre-existing immunity has proven challenging, particularly because a
547 strong antibody response against immunodominant epitopes that structurally surround
548 a subdominant neutralization epitope can sterically mask the neutralization epitope,
549 preventing a subdominant epitope from mounting a potent antibody response (*27, 29,*
550 *30, 60*). Overcoming immunodominance hierarchies under conditions of pre-existing

551 immunity has proven challenging both for RSV, Influenza, and others, and such
552 hierarchies seem to be impacted by multiple factors including serological antibody
553 levels, their specificity, memory B-cell counts, adjuvants, as well as the immunization
554 or infection route (*28*).
555
556 Heterologous prime-boost schemes are a promising strategy to guide the fine
557 specificity of antibody responses and to focus these responses on particularly
558 vulnerable antigenic sites. Several vaccine studies have been conducted for
559 pathogens such as Influenza (*37, 38*), RSV (*35*) and HIV (*32*), where the heterologous
560 immunogens were alternative strains or modified versions of the viral fusion proteins,
561 yet not heterologous to the same degree as a computationally designed, single epitope
562 scaffold. An important point to consider regarding immunogens based on modified
563 versions of viral proteins is whether immunodominant signatures do not actually
564 remain, and thereby steer the antibody responses away from the target epitopes.
565 While this scenario may not be fully absent in the synthetic epitope-scaffolds, it is at
566 least mitigated by the fact that the protein has not evolved under the pressure of
567 escaping the immune system.
568
569 Another key aspect in heterologous prime-boost schemes is to maintain the structural
570 integrity of the neutralizing epitope in both the priming and heterologous boosting
571 immunogens. FFL_001 has been thoroughly structurally characterized and presents
572 a very close mimicry of the site II epitope in RSVF (*21*). Importantly, a recent study by
573 Mousa et al. (*61*) has identified non-neutralizing antibodies that can compete with
574 Palivizumab by binding to a nearby epitope, and a large-scale sequence analysis has
575 suggested that the presence of similar antibodies may be common in the human RSV
576 immune response. However, as the site II epitope scaffold does not contain this non-
577 neutralizing site, their study demonstrated that FFL_001 can distinguish site II nAbs
578 from their non-neutralizing competitors (*61*). Using an extended panel of site II specific,
579 potent nAbs, we could confirm that the epitope scaffold binds with extremely high
580 affinity to multiple site II nAbs, leading us to speculate that NRM could recall site II-
581 specific memory B-cells *in vivo*, thereby boosting site II-specific serum titers. Given
582 the very low serum titers specific for antigenic site II following a prefusion RSVF prime,
583 it was questionable whether NRM could boost these subdominant antibody levels.
584 However, previous studies with HIV immunogens have shown that a very low number

585 of epitope-specific B-cells (1 out of 1,000,000) is sufficient to be selected and recruited
586 to the germinal center by a multimeric immunogen that binds with high affinity to the
587 target B-cell receptor (*57*). Indeed, we found that under conditions where site II-
588 specific antibodies are subdominant, a heterologous boost can redirect serum
589 antibody specificity towards increased site II recognition. Importantly, these antibodies
590 competed with Motavizumab for RSVF binding, confirming their recognition of the
591 epitope in its native quaternary context. In contrast, repeated immunization with
592 prefusion RSVF failed to direct antibodies towards antigenic site II.
593
594 This study demonstrates that the number of neutralization epitopes in a heterologous
595 boosting immunogen can be reduced to a single, well-defined site; which, if the
596 immunogen is optimally presented, can enhance pre-existing, subdominant antibody
597 responses targeting this epitope. The ability to narrowly focus antibody responses to
598 a single, well-understood epitope that mediates clinical protection once it is targeted
599 by sufficient antibody titers is an important milestone for RSV vaccine development.
600
601 Given that this approach is generalizable and that epitope scaffold nanoparticles have
602 proven successful in boosting nAbs specific for other sites, this strategy holds great
603 potential to tune levels of antibody specificities depending on the target population.
604 Goodwin et al. have shown that young infants preferentially develop RSV site III-
605 specific antibodies that lack somatic hypermutation (*48*). Consequently, vaccine
606 antigens given to pregnant women should primarily induce antibodies targeting
607 structurally distal antigenic sites in order to avoid interference with an immune
608 response mounted by the infant. Given these specific antibody lineage requirements
609 and the previously failed clinical trial in infants (*62*), its seems unlikely that a vaccine
610 based solely on prefusion RSVF could be maximally effective in all target populations.
611 The addition of precision immunogens to spotlight different antigenic sites tailored to
612 a specific patient population may increase the efficacy of prefusion RSVF-based
613 vaccines. An increasing structural and immunological understanding of antibody
614 specificities will help inform the design of novel immunogens and appropriate
615 immunization regimens, allowing the tailoring of vaccine-induced antibody responses
616 in different target populations.
617

618 However, our results show that the success of this boosting strategy is dependent on
619 the presence of a low but detectable amount of site II-specific antibodies elicited by
620 prefusion RSVF. Although three immunizations with NRM yielded even higher site II
621 peptide-specific antibodies, these antibodies were largely non-neutralizing. Further
622 studies in more relevant animal models will reveal if natural infection with RSV can
623 also serve as appropriate prime for subsequent boosting of site II-nAbs, as well as for
624 other RSV neutralization epitopes.
625
626 Projecting beyond the RSV vaccine problem, these results provide a strong rationale
627 for developing precision immunogens that present conserved, neutralization-sensitive
628 sites of other pathogens. For example, multiple epitopes on the Influenza
629 hemagglutinin head and stem region that confer broad and potent antibody-mediated
630 neutralization have been identified. Focusing antibody responses on these defined
631 epitopes may remove the need for annual vaccine reformulation, and may also protect
632 against emerging pandemic strains (*14, 51, 63, 64*). The Influenza vaccine challenge
633 seems particularly well suited to our approach considering that the human population
634 has pre-existing immunity to Influenza, including some subdominant bnAbs that
635 seasonal vaccines fail to stimulate (*27*). Additionally, antigenically related viruses such
636 as Zika and Dengue pose a major challenge for vaccine development, as antibodies
637 mounted against the envelope protein of a Dengue subtype can facilitate infection with
638 Zika (*65*) or other Dengue subtypes. A site conserved between all four Dengue
639 subtypes and Zika envelope protein has been structurally characterized and
640 suggested for the development of an epitope-focused immunogen (*7*).
641
642 When seeking to apply an immunofocusing strategy to other antigenic sites and
643 pathogens, one challenge is the development of epitope scaffolds stably presenting
644 the epitope in a synthetic immunogen that is compatible with antibody binding. While
645 the RSV antigenic site II is a structurally simple helix-turn-helix motif, many other
646 identified neutralization epitopes comprise multiple, discontinuous segments.
647 However, continuous advances in rational protein design techniques (*66*) will allow the
648 design of more complex protein scaffolds to stabilize increasingly complex epitopes.
649
650 Altogether, we have shown the development of an optimized RSV epitope scaffold
651 nanoparticle able to boost subdominant, neutralizing antibody responses *in vivo* that

652 target site II, an epitope of utmost clinical relevance. This is a distinctive feature
653 compared to using prefusion RSVF as a boosting immunogen, and underscores how
654 subdominant epitopes can be converted to immunodominant epitopes when
655 presented in a different environment. We foresee the great promise of this strategy to
656 overcome the challenge of boosting and focusing pre-existing immunity towards
657 defined neutralization epitopes, potentially applicable to multiple pathogens.
658
659 **Methods**
660
661 Resurfacing
662 The previously published RSV site II epitope scaffold ("FFL_001") (*21*) was designed
663 based on a crystal structure of a mutant of ribosome recycling factor from *E. coli* (PDB
664 entry 1ISE. Using BLAST, we identified sequence homologs of 1ISE from eukaryotic
665 organisms and created a multiple sequence alignment with clustal omega
666 (CLUSTALO (1.2.1)) (*67*) of the mouse homolog sequence (NCBI reference
667 NP_080698.1), 1ISE and FFL_001. Surface-exposed residues of FFL_001 were then
668 mutated to the respective residue of the mouse homolog using the Rosetta fixed
669 backbone design application (*43*), resulting in 38 surface mutations. Amino acid
670 changes were verified to not impact overall Rosetta energy score term.
671
672
673 Protein expression and purification
674 FFLM
675 DNA sequences of the epitope-scaffold designs were purchased from Genscript and
676 cloned in pET29b, in frame with a C-terminal 6x His tag. The plasmid was transformed
677 in *E. coli* BL21 (DE3) and grown in Terrific Broth supplemented with Kanamycin (50
678 µg/ml). Cultures were inoculated to an OD_{600} of 0.1 from an overnight culture and
679 incubated at 37°C. After reaching OD_{600} of 0.6, expression was induced by the addition
680 of 1 mM isopropyl-β-D-thiogalactoside (IPTG) and cells were incubated for further 4-
681 5h at 37°C. Cell pellets were resuspended in lysis buffer (50 mM TRIS, pH 7.5, 500
682 mM NaCl, 5% Glycerol, 1 mg/ml lysozyme, 1 mM PMSF, 1 µg/ml DNase) and
683 sonicated on ice for a total of 12 minutes, in intervals of 15 seconds sonication followed
684 by a 45 seconds pause. Lysates were clarified by centrifugation (18,000 rpm, 20
685 minutes), sterile-filtered and purified using a His-Trap FF column on an Äkta pure

686 system (GE healthcare). Bound proteins were eluted in buffer containing 50 mM Tris,
687 500 mM NaCl and 300 mM imidazole, pH 7.5. Concentrated proteins were further
688 purified by size exclusion chromatography on a Superdex™ 75 300/10 (GE
689 Healthcare) in PBS. Protein concentrations were determined via measuring the
690 absorbance at 280 nm on a Nanodrop (Thermo Scientific). Proteins were concentrated
691 by centrifugation (Millipore, #UFC900324) to 1 mg/ml, snap frozen in liquid nitrogen
692 and stored at -80°C.
693
694 NRM
695 The full-length N gene (sequence derived from the human RSV strain Long, ATCC
696 VR-26; GenBank accession number AY911262.1) was PCR amplified using the
697 Phusion DNA polymerase (Thermo Scientific) and cloned into pET28a+ at NcoI-XhoI
698 sites to obtain the pET-N plasmid. The sequence of FFLM was then PCR amplified
699 and cloned into pET-N at NcoI site to the pET-NRM plasmid. *E. coli* BL21 (DE3)
700 bacteria were co-transformed with pGEX-PCT (*68*) and pET-FFLM-N plasmids and
701 grown in LB medium containing ampicillin (100 µg/ml) and kanamycin (50 µg/ml). The
702 same volume of LB medium was then added, and protein expression was induced by
703 the addition of 0.33 mM IPTG to the medium. Bacteria were incubated for 15 h at 28°C
704 and then harvested by centrifugation. For protein purification, bacterial pellets were
705 resuspended in lysis buffer (50 mM Tris-HCl pH 7.8, 60 mM NaCl, 1 mM EDTA, 2 mM
706 dithiothreitol, 0.2% Triton X-100, 1 mg/ml lysozyme) supplemented with a complete
707 protease inhibitor cocktail (Roche), incubated for one hour on ice, and disrupted by
708 sonication. The soluble fraction was collected by centrifugation at 4 °C for 30 min at
709 10,000 x g. Glutathione-Sepharose 4B beads (GE Healthcare) were added to clarify
710 supernatants and incubated at 4°C for 15h. The beads were then washed one time in
711 lysis buffer and two times in 20 mM Tris pH 8.5, 150 mM NaCl. To isolate NRM, beads
712 containing bound complex were incubated with thrombine for 16 h at 20 °C. After
713 cleavage of the GST tag, the supernantant was loaded onto a Sephacryl S-200 HR
714 16/30 column (GE Healthcare) and eluted in 20 mM Tris-HCl, 150 mM NaCl, pH 8.5.
715
716 Antibody variable fragments (Fabs)
717 For Fab expression, heavy and light chain DNA sequences were purchased from Twist
718 Biosciences and cloned separately into the pHLSec mammalian expression vector
719 (Addgene, #99845) using AgeI and XhoI restriction sites. Expression plasmids were

720 pre-mixed in a 1:1 stoichiometric ratio, co-transfected into HEK293-F cells and
721 cultured in FreeStyle™ medium (Gibco, #12338018). Supernatants were harvested
722 after one week by centrifugation and purified using a kappa-select column (GE
723 Healthcare). Elution of bound proteins was conducted using 0.1 M glycine buffer (pH
724 2.7) and eluates were immediately neutralized by the addition of 1 M Tris ethylamine
725 (pH 9), followed by buffer exchange to PBS pH 7.4.
726
727 Respiratory Syncytial Virus Fusion protein (prefusion RSVF)
728 Protein sequence of prefusion RSVF corresponds to the sc9-10 DS-Cav1 A149C
729 Y458C S46G E92D S215P K465Q variant designed by Joyce et al. (*45*), which we
730 refer to as RSVF DS2. RSVF DS2 was codon optimized for mammalian expression
731 and cloned into the pHCMV-1 vector together with two C-terminal Strep-Tag II and
732 one 8x His tag. Plasmids were transfected in HEK293-F cells and cultured in
733 FreeStyle™ medium. Supernatants were harvested one week after transfection and
734 purified via Ni-NTA affinity chromatography. Bound protein was eluted using buffer
735 containing 10 mM Tris, 500 mM NaCl and 300 mM Imidazole (pH 7.5), and eluate was
736 further purified on a StrepTrap HP affinity column (GE Healthcare). Bound protein was
737 eluted in 10mM Tris, 150 mM NaCl and 20 mM Desthiobiotin (Sigma), pH 8, and size
738 excluded in PBS, pH 7.4, on a Superdex 200 Increase 10/300 GL column (GE
739 Healthcare) to obtain trimeric RSVF.
740
741 Affinity determination using Surface Plasmon Resonance
742 Surface Plasmon Resonance experiments were performed on a Biacore 8K at room
743 temperature with HBS-EP+ running buffer (10 mM HEPES pH 7.4, 150 mM NaCl, 3
744 mM EDTA, 0.005 % v/v Surfactant P20) (GE Healthcare). Approximately 100
745 response units (RU) of FFLM were immobilized via amine coupling on a CM5 sensor
746 chip (GE Healthcare). Serial dilutions of site II-specific antibody variable fragments
747 (fabs) were injected as analyte at a flow rate of 30 µl/min with 120 seconds contact
748 time. Following each injection cycle, ligand regeneration was performed using 0.1 M
749 glycine, pH 2. Data analysis was performed using 1:1 Langmuir binding kinetic fits
750 within the Biacore evaluation software (GE Healthcare).
751
752 Mouse immunizations

753 All animal experiments were approved by the Veterinary Authority of the Canton of
754 Vaud (Switzerland) according to Swiss regulations of animal welfare (animal protocol
755 number 3074). Six-week-old, female Balb/c mice were ordered from Janvier labs and
756 acclimatized for one week. Immunogens were thawed on ice and diluted in PBS pH
757 7.4 to a concentration of 0.2 mg/ml. The immunogens were then mixed with an equal
758 volume of 2% Alhydrogel® (Invivogen), resulting in a final Alhydrogel concentration
759 of 1%. Other adjuvants were formulated according to manufacturer's instructions.
760 After mixing immunogens and adjuvants for one hour at 4°C, each mouse was
761 injected with 100 μl, corresponding to 10 μg immunogen adsorbed to Alhydrogel. All
762 immunizations were done subcutaneously, with no visible irritation around the
763 injection site. Immunizations were performed on day 0, 21 and 42. 100-200 μl blood
764 were drawn on day 0, 14, 35, and the maximum amount of blood (200-1000μl) was
765 taken by cardiac puncture at day 56, when mice were sacrificed.
766
767 Antigen ELISA
768 Nunc Medisorp plates (Thermo Scientific, # 467320) were coated overnight at 4°C with
769 100 μl of antigen (recombinant RSVF, FFLM and NRM) diluted in coating buffer (100
770 mM sodium bicarbonate, pH 9) at a final concentration of 0.5 μg/ml. For blocking,
771 plates were incubated for two hours at room temperature with blocking buffer (PBS +
772 0.05% Tween 20 (PBST) supplemented with 5% skim milk powder (Sigma, #70166)).
773 Mouse sera were serially diluted in blocking buffer and incubated for one hour at room
774 temperature. Plates were washed five times with PBST before adding 100 μl of anti-
775 mouse HRP-conjugated secondary antibody diluted at 1:1500 in blocking buffer
776 (abcam, #ab99617). An additional five washes were performed before adding Pierce
777 TMB substrate (Thermo Scientific, # 34021). The reaction was stopped by adding 100
778 μl of 2M sulfuric acid, and absorbance at 450 nm was measured on a Tecan Safire 2
779 plate reader.
780 Each plate contained a standard curve of Motavizumab to normalize signals between
781 different plates and experiments. Normalization was done in GraphPad Prism. The
782 mean value was plotted for each cohort and statistical analysis was performed using
783 GraphPad Prism.
784
785 Competition ELISA

786 Prior to incubation with a coated antigen plate, sera were serially diluted in the
787 presence of 100 μg/ml competitor antigen and incubated overnight at 4°C. ELISA
788 curves of a positive control, Motavizumab, are shown in Supplementary Figure 6.
789 Curves were plotted using GraphPad Prism, and the area under the curve (AUC) was
790 calculated for the specific (NRM) and control (RSVN) competitor. % competition was
791 calculated using the following formula (*69*):
792
793 $$\% \text{ competition} = \left(1 - \left(\frac{AUC(specific\ competitor\ (NRM))}{AUC(control\ competitor\ (NR))}\right)\right) * 100$$
794
795 Peptide sandwich ELISA
796 The antigenic site II was synthesized as peptide by JPT Peptide Technologies,
797 Germany. The following sequence was synthesized and biotinylated at the N-
798 terminus:
799 MLTNSELLSKINDMPITNDQKKLMSNNVQI
800 For ELISA analysis of peptide-reactive serum antibodies, Nunc MediSorp plates were
801 coated with 5 μg/ml streptavidin (Thermo Scientific, #21122) for one hour at 37°C.
802 Subsequently, ELISA plates were blocked as indicated above, followed by the addition
803 of 2.4 μg/ml of the biotinylated site II peptide. Coupling was performed for one hour at
804 room temperature. The subsequent steps were performed as described for the antigen
805 ELISA.
806
807 Serum competition using Surface Plasmon Resonance
808 Approximately 300 RU of antigen were immobilized via amine coupling on a CM5 chip.
809 Mouse sera were diluted 1:100 in HBS-EP+ running buffer and flowed as analyte with
810 a contact time of 120 seconds to obtain an initial response unit ($RU_{non\text{-}blocked\ surface}$).
811 The surface was regenerated using 50 mM NaOH. Sequentially, Motavizumab was
812 injected four times at a concentration of 2 μM, leading to complete blocking of
813 Motavizumab binding sites as confirmed by signal saturation. The same serum dilution
814 was reinjected to determine the remaining response ($RU_{blocked\ surface}$). The delta serum
815 response (ΔSR) corresponds to the baseline-subtracted, maximum signal of the
816 injected sera.
817
818 $$\Delta \mathrm{SR} = \mathrm{RU}_{(\mathrm{non-})\mathrm{blocked\ surface}} - \mathrm{RU}_{\mathrm{Baseline}}$$

819

820 Percent blocking was calculated as follows:

821

822 $$\% \text{ blocking} = (1 - (\frac{\Delta \text{ SR}_{\text{blocked surface}}}{\Delta \text{ SR}_{\text{non-blocked surface}}})) * 100$$

823

824 A schematic representation of the SPR experiment is shown in Supplementary Figure
825 7, and calculated blocking values are shown in Supplementary Table 1.

826

827 Enzyme-linked immunospot assay (ELISPOT)

828 B-cell ELISPOT assays were performed using the Mouse IgG ELISpot HRP kit
829 (Mabtech, #3825-2H) according to the manufacturer's instructions. Briefly, mouse
830 spleens were isolated, and pressed through a cell strainer (Corning, #352350) to
831 obtain a single cell suspension. Splenocytes were resuspended in RPMI media
832 (Gibco, #11875093) supplemented with 10% FBS (Gibco), Penicillin/Streptomycin
833 (Gibco), 0.01 µg/ml IL2, 1 µg/ml R848 (Mabtech, #3825-2H) and 50 µM β-
834 mercaptoethanol (Sigma) for ~60 hours stimulation at 37 °C, 5% CO_2. ELISpot plates
835 (PVDF 96-well plates, Millipore, #MSIPS4510) were coated overnight with 15 µg/ml
836 antigen diluted in PBS, followed by careful washing and blocking using RPMI + 10%
837 FBS. Live splenocytes were counted and the cell number was adjusted to $1x10^7$
838 cells/ml. Serial dilutions of splenocytes were plated in duplicates and incubated
839 overnight with coated plates. After several wash steps with PBS buffer, plates were
840 incubated for two hours with biotinylated anti-mouse total IgG (Mabtech, # 3825-6-
841 250) in PBS, followed by incubation with streptavidin-conjugated to HRP (Mabtech,
842 #3310-9) for one hour. Spots were revealed using tetramethylbenzidine (TMB,
843 Mabtech, #3651-10) and counted with an automatic reader (Bioreader 2000; BioSys
844 GmbH). Results were represented as number of spots per 10^6 splenocytes.

845

846 RSV neutralization assay

847 The RSV A2 strain carrying a luciferase gene (RSV-Luc) was a kind gift of Marie-Anne
848 Rameix-Welti, UFR des Sciences et de la Santé, Paris. Hep2 cells were seeded in
849 Corning 96-well tissue culture plates (Sigma, #CLS3595) at a density of 40,000
850 cells/well in 100 µl of Minimum Essential Medium (MEM, Gibco, #11095-080)

851 supplemented with 10% FBS (Gibco, 10500-084), L-glutamine 2 mM (Gibco, #25030-
852 081) and penicillin-streptomycin (Gibco, #15140-122), and grown overnight at 37 °C
853 with 5% CO2.
854 Sera were heat-inactivated for 30 minutes at 56 °C. Serial two-fold dilutions were
855 prepared in an untreated 96-well plate using MEM without phenol red (M0, Life
856 Technologies, #51200-038) containing 2mM L-glutamine, penicillin + streptomycin,
857 and mixed with 800 pfu/well RSV-Luc (corresponding to a final MOI of 0.01). After
858 incubating diluted sera and virus for one hour at 37 °C, growth media was removed
859 from the Hep2 cell layer and 100 μl/well of the serum-virus mixture added. After 48
860 hours, cells were lysed in 100 µl buffer containing 32 mM Tris pH 7.9, 10 mM $MgCl_2$,
861 1.25% Triton X-100, 18.75% glycerol and 1mM DTT. 50 µl lysate were transferred to
862 a 96-well plate with white background (Sigma, # CLS3912). 50 µl of lysis buffer
863 supplemented with 1 µg/ml luciferin (Sigma, #L-6882) and 2 mM ATP (Sigma, #A3377)
864 were added to each well immediately before reading luminescence signal on a Tecan
865 Infinite 500 plate reader.
866 On each plate, a Palivizumab dilution series was included to ensure comparability of
867 neutralization data. In our assay, we determined IC_{50} values for Palivizumab of 0.32
868 µg/ml, which is similar to what other groups have reported (*44*). The neutralization
869 curve was plotted and fitted using the GraphPad variable slope fitting model, weighted
870 by $1/Y^2$.
871
872 Sera fractionation
873 400 µl of streptavidin agarose beads (Thermo Scientific, #20347) were pelleted at
874 13,000 rpm for 2 minutes in a table top centrifuge and washed with phosphate buffered
875 saline (PBS). 200 µg of biotinylated site II peptide were incubated for 2 hours at room
876 temperature to allow coupling of biotinylated peptide to streptavidin beads. Beads
877 were washed three times with 1 ml PBS to remove excess of peptide and resuspended
878 to a total volume of 500 µl bead slurry. Mouse sera from the same cohort (n=10) were
879 pooled (4 µl each, 40 µl total) in a total volume of 200 µl PBS, and 90 µl diluted sera
880 were mixed with 150 µl of bead slurry, followed by an overnight incubation at 4 °C.
881 Beads were pelleted by centrifugation and the supernatant carefully removed by
882 pipetting. Beads were then washed twice with 200 µl PBS and the wash fractions were
883 discarded. To elute site II-specific antibodies, beads were resuspended in 200 µl

884 elution buffer (0.1 M glycine, pH 2.7) and incubated for 1 minute before centrifugation.
885 Supernatant was removed, neutralized with 40 µl neutralization buffer (1 M Tris pH
886 7.5, 300 mM NaCl), and stored at -20 °C for subsequent testing for RSV neutralization.
887 As a control, unconjugated streptavidin was used for each sample to account for non-
888 specific binding.
889
890 Next-generation antibody repertoire sequencing (NGS)
891 RNA isolation
892 Mouse bone marrow was isolated from femurs and re-suspended in 1.5 ml Trizol (Life
893 Technologies, #15596) and stored at -80˚C until further processing. RNA extraction
894 was performed using the PureLink RNA Mini Kit (Life Technologies, #12183018A)
895 following the manufacturer guidelines.
896
897 Antibody sequencing library preparation
898 Library preparation for antibody variable heavy chain regions was performed using a
899 protocol that incorporates unique molecular identifier (UID) tagging, as previously
900 described in Khan *et al.* (*70*). Briefly, first-strand cDNA synthesis was performed by
901 using Maxima reverse transcriptase (Life Technologies, #EP0742) following the
902 manufacturer instructions, using 5 µg RNA with 20 pmol of IgG gene-specific primers
903 (binding IgG1, IgG2a, IgG2b, IgG2c, and IgG3) with an overhang of a reverse UID
904 (RID). After cDNA synthesis, samples were subjected to a left-hand sided SPRIselect
905 bead (Beckman Coulter, #B23318) cleanup at 0.8X. Quantification of target-specific
906 cDNA by a digital droplet (dd)PCR assay allowed exact input of 135000 copies into
907 the next PCR step. Reaction mixtures contained a forward multiplex primer set that
908 was specific for variable heavy region framework 1 and possessed forward UID (FID),
909 a 3' Illumina adapter specific reverse primer, and 1X KAPA HIFI HotStart Uracil+
910 ReadyMix (KAPA Biosystems, #KK2802). PCR reactions were then left-hand side
911 SPRIselect bead cleaned as before and quantified using ddPCR assay. Finally, an
912 Illumina adaptor-extension PCR step was carried out using 820000 copies of the
913 previous PCR product. Following 2nd-step adaptor-extension PCR, reactions were
914 cleaned using a double-sided SPRIselect bead cleanup process (0.5X-0.8X) and
915 eluted in TE buffer.
916

917 NGS with Illumina MiSeq (2 x 300 bp)
918 After library preparation, individual NGS libraries were characterized for quality and
919 quantified by capillary electrophoresis using a Fragment Analyzer (Advanced
920 Analytical DNF-473 Standard Sensitivity). Samples were then pooled and NGS was
921 performed on the Illumina MiSeq platform with a MiSeq Reagent Kit V3, 2x300bp
922 paired-end (Illumina, #MS-102-3003), using an input concentration of 10 pM with 10%
923 PhiX.
924
925 Error and bias correction
926 Error and bias correction was performed using molecular amplification fingerprinting
927 pipeline, as previously described (*70, 71*).
928 1) Bioinformatic preprocessing
929 Paired-end FASTQ files obtained from Illumina MiSeq were imported into CLC
930 Genomics Workbench 10 on the ETH Zurich Euler High Performance Computing
931 (HPC) cluster. A preprocessing workflow was run containing the following steps:
932 trimming of low quality reads, merging of paired-end reads, removal of sequences not
933 aligning to mouse IGH constant sequences, and length filtering.
934
935 2) Error correction by consensus building
936 After pre-processing all datasets were downsampled to contain the same amount of
937 sequencing reads as the dataset with the lowest overall number of reads (361749
938 sequencing reads). For error correction, a custom Python script was used to perform
939 consensus building on the sequences for which at least three reads per UID were
940 required. VDJ annotation and frequency calculation was then performed by our in-
941 house aligner (*70, 71*). The complete error-correction and alignment pipeline is
942 available under https://gitlab.ethz.ch/reddy/MAF.
943
944 Sequence analysis and data visualization
945 Data analysis was done by customized scripts in R. For the identification of clonotypes
946 hierarchical clustering (*71*) was utilized to group CDR3 sequences together. The
947 following parameters were used: identical IGHV and IGHJ gene segment usage,
948 identical CDR3 length, and at least 80% CDR3 amino acid similarity to one other
949 sequence in the given clonotype (single linkage). The overlap of clonotypes between
950 both cohorts was analyzed by extracting the 20 most expanded clonotypes from each

951 cohort and visualizing their size, occurrence, and Vgene usage by a circos plot using
952 R software circlize (*72*). CDR3 sequence similarities between overlapping clonotypes
953 were represented graphically with the R software motifStack (*73*). Scripts used for
954 analysis are available under https://github.com/luciacsep/EpitopeFocussing.
955

956 **Data availability**

957 Data supporting the findings of this study are available within the article and its
958 Supplementary Information, or are available from the authors upon request.

959 **Contributions**

960 F.S. and B.E.C. designed experiments. M.G. expressed and purified RSVN and NRM
961 fusion protein. F.S., C.Y., S.S.V and P.C performed ELISAs. F.S. designed and
962 performed SPR competition assay. F.S., C.Y and P.C performed ELISpot
963 experiments, S.S.V, P.C and S.R performed mouse immunizations. L.C and S.F
964 performed next generation sequencing analysis. F.S., J.B. and P.G. designed FFLM.
965 F.S., P.C and M.C. performed RSV neutralization assay. F.S. and B.E.C wrote the
966 paper. All authors commented on the manuscript.
967

968 **Acknowledgements**

969 We thank Stefan Kunz for helpful discussions and critical reading of the manuscript.
970 This work was supported by the Swiss initiative for systems biology (SystemsX.ch),
971 the European Research Council (Starting grant - 716058) and the Swiss National
972 Science Foundation.
973

974 **Competing interests**

975 The authors declare no competing financial interests.
976

977 **References**

978 1. R. Rappuoli, C. W. Mandl, S. Black, E. De Gregorio, Vaccines for the twenty-first
979 century society. *Nat Rev Immunol* **11**, 865-872 (2011).
980 2. S. A. Plotkin, Correlates of protection induced by vaccination. *Clin Vaccine Immunol*
981 **17**, 1055-1065 (2010).
982 3. D. R. Burton, L. Hangartner, Broadly Neutralizing Antibodies to HIV and Their Role in
983 Vaccine Design. *Annu Rev Immunol* **34**, 635-659 (2016).

984 4. P. S. Lee, I. A. Wilson, Structural characterization of viral epitopes recognized by
985 broadly cross-reactive antibodies. *Curr Top Microbiol Immunol* **386**, 323-341 (2015).
986 5. M. S. Gilman *et al.*, Rapid profiling of RSV antibody repertoires from the memory B
987 cells of naturally infected adult donors. *Sci Immunol* **1**, (2016).
988 6. J. S. McLellan, Neutralizing epitopes on the respiratory syncytial virus fusion
989 glycoprotein. *Curr Opin Virol* **11**, 70-75 (2015).
990 7. G. Barba-Spaeth *et al.*, Structural basis of potent Zika-dengue virus antibody cross-
991 neutralization. *Nature* **536**, 48-53 (2016).
992 8. D. F. Robbiani *et al.*, Recurrent Potent Human Neutralizing Antibodies to Zika Virus in
993 Brazil and Mexico. *Cell* **169**, 597-609 e511 (2017).
994 9. M. Xu *et al.*, A potent neutralizing antibody with therapeutic potential against all
995 four serotypes of dengue virus. *NPJ Vaccines* **2**, 2 (2017).
996 10. Z. A. Bornholdt *et al.*, Isolation of potent neutralizing antibodies from a survivor of
997 the 2014 Ebola virus outbreak. *Science* **351**, 1078-1083 (2016).
998 11. S. Chandramouli *et al.*, Structural basis for potent antibody-mediated neutralization
999 of human cytomegalovirus. *Sci Immunol* **2**, (2017).
1000 12. K. M. Hastie *et al.*, Structural basis for antibody-mediated neutralization of Lassa
1001 virus. *Science* **356**, 923-928 (2017).
1002 13. S. C. Harrison, Viral membrane fusion. *Virology* **479-480**, 498-507 (2015).
1003 14. D. Corti *et al.*, A neutralizing antibody selected from plasma cells that binds to group
1004 1 and group 2 influenza A hemagglutinins. *Science* **333**, 850-856 (2011).
1005 15. J. S. McLellan *et al.*, Structure of RSV fusion glycoprotein trimer bound to a
1006 prefusion-specific neutralizing antibody. *Science* **340**, 1113-1117 (2013).
1007 16. D. R. Burton, Antibodies, viruses and vaccines. *Nat Rev Immunol* **2**, 706-713 (2002).
1008 17. D. R. Burton, What Are the Most Powerful Immunogen Design Vaccine Strategies?
1009 Reverse Vaccinology 2.0 Shows Great Promise. *Cold Spring Harb Perspect Biol* **9**,
1010 (2017).
1011 18. J. S. McLellan *et al.*, Structure-based design of a fusion glycoprotein vaccine for
1012 respiratory syncytial virus. *Science* **342**, 592-598 (2013).
1013 19. A. Impagliazzo *et al.*, A stable trimeric influenza hemagglutinin stem as a broadly
1014 protective immunogen. *Science* **349**, 1301-1306 (2015).
1015 20. H. M. Yassine *et al.*, Hemagglutinin-stem nanoparticles generate heterosubtypic
1016 influenza protection. *Nat Med* **21**, 1065-1070 (2015).
1017 21. B. E. Correia *et al.*, Proof of principle for epitope-focused vaccine design. *Nature* **507**,
1018 201-206 (2014).
1019 22. M. F. Delgado *et al.*, Lack of antibody affinity maturation due to poor Toll-like
1020 receptor stimulation leads to enhanced respiratory syncytial virus disease. *Nat Med*
1021 **15**, 34-41 (2009).
1022 23. A. M. Killikelly, M. Kanekiyo, B. S. Graham, Pre-fusion F is absent on the surface of
1023 formalin-inactivated respiratory syncytial virus. *Sci Rep* **6**, 34108 (2016).
1024 24. I. Widjaja *et al.*, Characterization of Epitope-Specific Anti-Respiratory Syncytial Virus
1025 (Anti-RSV) Antibody Responses after Natural Infection and after Vaccination with
1026 Formalin-Inactivated RSV. *J Virol* **90**, 5965-5977 (2016).
1027 25. R. T. Stein *et al.*, Respiratory syncytial virus hospitalization and mortality: Systematic
1028 review and meta-analysis. *Pediatr Pulmonol* **52**, 556-569 (2017).
1029 26. B. B. Finlay, G. McFadden, Anti-immunology: evasion of the host immune system by
1030 bacterial and viral pathogens. *Cell* **124**, 767-782 (2006).

1031 27. S. F. Andrews *et al.*, Immune history profoundly affects broadly protective B cell
1032 responses to influenza. *Sci Transl Med* **7**, 316ra192 (2015).
1033 28. D. Angeletti *et al.*, Defining B cell immunodominance to viruses. *Nat Immunol* **18**,
1034 456-463 (2017).
1035 29. V. I. Zarnitsyna *et al.*, Masking of antigenic epitopes by antibodies shapes the
1036 humoral immune response to influenza. *Philos Trans R Soc Lond B Biol Sci* **370**,
1037 (2015).
1038 30. V. I. Zarnitsyna, J. Lavine, A. Ellebedy, R. Ahmed, R. Antia, Multi-epitope Models
1039 Explain How Pre-existing Antibodies Affect the Generation of Broadly Protective
1040 Responses to Influenza. *PLoS Pathog* **12**, e1005692 (2016).
1041 31. G. D. Victora, M. C. Nussenzweig, Germinal centers. *Annu Rev Immunol* **30**, 429-457
1042 (2012).
1043 32. B. Briney *et al.*, Tailored Immunogens Direct Affinity Maturation toward HIV
1044 Neutralizing Antibodies. *Cell* **166**, 1459-1470 e1411 (2016).
1045 33. J. G. Jardine *et al.*, HIV-1 VACCINES. Priming a broadly neutralizing antibody response
1046 to HIV-1 using a germline-targeting immunogen. *Science* **349**, 156-161 (2015).
1047 34. M. Silva *et al.*, Targeted Elimination of Immunodominant B Cells Drives the Germinal
1048 Center Reaction toward Subdominant Epitopes. *Cell Rep* **21**, 3672-3680 (2017).
1049 35. J. C. Boyington *et al.*, Structure-Based Design of Head-Only Fusion Glycoprotein
1050 Immunogens for Respiratory Syncytial Virus. *PLoS One* **11**, e0159709 (2016).
1051 36. G. A. Kirchenbaum, D. M. Carter, T. M. Ross, Sequential Infection in Ferrets with
1052 Antigenically Distinct Seasonal H1N1 Influenza Viruses Boosts Hemagglutinin Stalk-
1053 Specific Antibodies. *J Virol* **90**, 1116-1128 (2016).
1054 37. K. Van Reeth *et al.*, Heterologous prime-boost vaccination with H3N2 influenza
1055 viruses of swine favors cross-clade antibody responses and protection. *NPJ Vaccines*
1056 **2**, (2017).
1057 38. C. J. Wei *et al.*, Induction of broadly neutralizing H1N1 influenza antibodies by
1058 vaccination. *Science* **329**, 1060-1064 (2010).
1059 39. P. L. Herve *et al.*, RSV N-nanorings fused to palivizumab-targeted neutralizing
1060 epitope as a nanoparticle RSV vaccine. *Nanomedicine* **13**, 411-420 (2017).
1061 40. X. Roux *et al.*, Sub-nucleocapsid nanoparticles: a nasal vaccine against respiratory
1062 syncytial virus. *PLoS One* **3**, e1766 (2008).
1063 41. R. G. Tawar *et al.*, Crystal structure of a nucleocapsid-like nucleoprotein-RNA
1064 complex of respiratory syncytial virus. *Science* **326**, 1279-1283 (2009).
1065 42. B. E. Correia *et al.*, Computational protein design using flexible backbone remodeling
1066 and resurfacing: case studies in structure-based antigen design. *J Mol Biol* **405**, 284-
1067 297 (2011).
1068 43. B. Kuhlman, D. Baker, Native protein sequences are close to optimal for their
1069 structures. *Proc Natl Acad Sci U S A* **97**, 10383-10388 (2000).
1070 44. H. Wu *et al.*, Development of motavizumab, an ultra-potent antibody for the
1071 prevention of respiratory syncytial virus infection in the upper and lower respiratory
1072 tract. *J Mol Biol* **368**, 652-665 (2007).
1073 45. M. G. Joyce *et al.*, Iterative structure-based improvement of a fusion-glycoprotein
1074 vaccine against RSV. *Nat Struct Mol Biol* **23**, 811-820 (2016).
1075 46. J. L. Xu, M. M. Davis, Diversity in the CDR3 region of V(H) is sufficient for most
1076 antibody specificities. *Immunity* **13**, 37-45 (2000).

1077 47. J. F. Scheid *et al.*, Sequence and structural convergence of broad and potent HIV
1078 antibodies that mimic CD4 binding. *Science* **333**, 1633-1637 (2011).
1079 48. E. Goodwin *et al.*, Infants Infected with Respiratory Syncytial Virus Generate Potent
1080 Neutralizing Antibodies that Lack Somatic Hypermutation. *Immunity* **48**, 339-349
1081 e335 (2018).
1082 49. S. Friedensohn, T. A. Khan, S. T. Reddy, Advanced Methodologies in High-Throughput
1083 Sequencing of Immune Repertoires. *Trends Biotechnol* **35**, 203-214 (2017).
1084 50. L. J. Anderson *et al.*, Strategic priorities for respiratory syncytial virus (RSV) vaccine
1085 development. *Vaccine* **31 Suppl 2**, B209-215 (2013).
1086 51. N. L. Kallewaard *et al.*, Structure and Function Analysis of an Antibody Recognizing
1087 All Influenza A Subtypes. *Cell* **166**, 596-608 (2016).
1088 52. I. Rossey, J. S. McLellan, X. Saelens, B. Schepens, Clinical Potential of Prefusion RSV F-
1089 specific Antibodies. *Trends Microbiol* **26**, 209-219 (2018).
1090 53. A. Mejias, O. Ramilo, Review of palivizumab in the prophylaxis of respiratory
1091 syncytial virus (RSV) in high-risk infants. *Biologics* **2**, 433-439 (2008).
1092 54. G. Ofek *et al.*, Elicitation of structure-specific antibodies by epitope scaffolds. *Proc*
1093 *Natl Acad Sci U S A* **107**, 17880-17887 (2010).
1094 55. N. Jaberolansar *et al.*, Induction of high titred, non-neutralising antibodies by self-
1095 adjuvanting peptide epitopes derived from the respiratory syncytial virus fusion
1096 protein. *Sci Rep* **7**, 11130 (2017).
1097 56. J. S. McLellan *et al.*, Design and characterization of epitope-scaffold immunogens
1098 that present the motavizumab epitope from respiratory syncytial virus. *J Mol Biol*
1099 **409**, 853-866 (2011).
1100 57. R. K. Abbott *et al.*, Precursor Frequency and Affinity Determine B Cell Competitive
1101 Fitness in Germinal Centers, Tested with Germline-Targeting HIV Vaccine
1102 Immunogens. *Immunity* **48**, 133-146 e136 (2018).
1103 58. B. E. Correia *et al.*, Computational design of epitope-scaffolds allows induction of
1104 antibodies specific for a poorly immunogenic HIV vaccine epitope. *Structure* **18**,
1105 1116-1126 (2010).
1106 59. J. O. Ngwuta *et al.*, Prefusion F-specific antibodies determine the magnitude of RSV
1107 neutralizing activity in human sera. *Sci Transl Med* **7**, 309ra162 (2015).
1108 60. S. F. Andrews *et al.*, High preexisting serological antibody levels correlate with
1109 diversification of the influenza vaccine response. *J Virol* **89**, 3308-3317 (2015).
1110 61. J. J. Mousa *et al.*, Structural basis for nonneutralizing antibody competition at
1111 antigenic site II of the respiratory syncytial virus fusion protein. *Proc Natl Acad Sci U*
1112 *S A* **113**, E6849-E6858 (2016).
1113 62. H. W. Kim *et al.*, Respiratory syncytial virus disease in infants despite prior
1114 administration of antigenic inactivated vaccine. *Am J Epidemiol* **89**, 422-434 (1969).
1115 63. D. C. Ekiert *et al.*, A highly conserved neutralizing epitope on group 2 influenza A
1116 viruses. *Science* **333**, 843-850 (2011).
1117 64. D. D. Raymond *et al.*, Conserved epitope on influenza-virus hemagglutinin head
1118 defined by a vaccine-induced antibody. *Proc Natl Acad Sci U S A* **115**, 168-173 (2018).
1119 65. W. Dejnirattisai *et al.*, Dengue virus sero-cross-reactivity drives antibody-dependent
1120 enhancement of infection with zika virus. *Nat Immunol* **17**, 1102-1108 (2016).
1121 66. A. Chevalier *et al.*, Massively parallel de novo protein design for targeted
1122 therapeutics. *Nature* **550**, 74-79 (2017).

1123 67. F. Sievers *et al.*, Fast, scalable generation of high-quality protein multiple sequence
1124 alignments using Clustal Omega. *Mol Syst Biol* **7**, 539 (2011).
1125 68. N. Castagne *et al.*, Biochemical characterization of the respiratory syncytial virus P-P
1126 and P-N protein complexes and localization of the P protein oligomerization domain.
1127 *J Gen Virol* **85**, 1643-1653 (2004).
1128 69. D. W. Kulp *et al.*, Structure-based design of native-like HIV-1 envelope trimers to
1129 silence non-neutralizing epitopes and eliminate CD4 binding. *Nat Commun* **8**, 1655
1130 (2017).
1131 70. T. A. Khan *et al.*, Accurate and predictive antibody repertoire profiling by molecular
1132 amplification fingerprinting. *Sci Adv* **2**, e1501371 (2016).
1133 71. S. Friedensohn *et al.*, Synthetic Standards Combined With Error and Bias Correction
1134 Improve the Accuracy and Quantitative Resolution of Antibody Repertoire
1135 Sequencing in Human Naive and Memory B Cells. *Front Immunol* **9**, 1401 (2018).
1136 72. Z. Gu, L. Gu, R. Eils, M. Schlesner, B. Brors, circlize Implements and enhances circular
1137 visualization in R. *Bioinformatics* **30**, 2811-2812 (2014).
1138 73. J. Ou, S. A. Wolfe, M. H. Brodsky, L. J. Zhu, motifStack for the analysis of transcription
1139 factor binding site evolution. *Nat Methods* **15**, 8-9 (2018).
1140